HHS Public Access

Author manuscript

Neurobiol Dis. Author manuscript; available in PMC 2017 September 01.

Published in final edited form as:

Neurobiol Dis. 2016 September ; 93: 1–11. doi:10.1016/j.nbd.2016.03.022.

The polarity protein Par3 regulates APP trafficking and processing through the endocytic adaptor protein Numb

Miao Sun, **Suwaiba Z. Asghar**, and **Huaye Zhang***

Department of Neuroscience and Cell Biology, Robert Wood Johnson Medical School, Rutgers, the State University of New Jersey, Piscataway, NJ 08854

Abstract

The processing of amyloid precursor protein (APP) into β-amyloid peptide (Aβ) is a key step in the pathogenesis of Alzheimer's disease (AD), and trafficking dysregulations of APP and its secretases contribute significantly to altered APP processing. Here we show that the cell polarity protein Par3 plays an important role in APP processing and trafficking. We found that the expression of full length Par3 is significantly decreased in AD patients. Overexpression of Par3 promotes non-amyloidogenic APP processing while depletion of Par3 induces intracellular accumulation of Aβ. We further show that Par3 functions by regulating APP trafficking. Loss of Par3 decreases surface expression of APP by targeting APP to the late endosome/lysosome pathway. Finally, we show that the effects of Par3 are mediated through the endocytic adaptor protein Numb, and Par3 functions by interfering with the interaction between Numb and APP. Together, our studies show a novel role for Par3 in regulating APP processing and trafficking.

Keywords

cell polarity; trafficking; Alzheimer disease; amyloid precursor protein (APP); amyloid-β (Aβ); Par3; Numb

Introduction

Alzheimer's disease (AD) is a devastating age-related neurodegenerative disease. Of the AD cases, over 90% are sporadic and advanced age remains the biggest risk factor. AD is characterized by the presence of β-amyloid (Aβ) plaques and neurofibrillary tangles containing hyperphosphorylated tau. Aβ is generated by β- and γ-secretase cleavage of the

*To whom correspondence should be addressed: Department of Neuroscience and Cell Biology, Rutgers Robert Wood Johnson Medical School, Piscataway, NJ 08854, huaye.zhang@rutgers.edu.

Conflict of Interest

The authors declare that they have no conflicts of interest with the contents of this article.

Author Contributions

MS and HZ designed the experiments and wrote the manuscript. MS performed experiments and analyzed the data. SZA performed experiments. All authors reviewed the results and approved the final version of the manuscript.

single-transmembrane amyloid precursor protein (APP). APP can also be processed by α-secretase, which cleaves within Aβ. A non-toxic P3 peptide is generated instead. Thus, channeling APP processing towards this non-amyloidogenic pathway can reduce Aβ production and potentially slow down AD progression (1). Significant evidence shows that the trafficking properties of both APP and its secretases affects how APP is processed (2). It is generally believed that amyloidogenic processing occurs in the endocytic compartments, where β- and γ-secretases show optimal activity (3,4). By contrast, non-amyloidogenic processing occurs mostly on the cell surface (5). It is thus important to understand the molecular mechanisms regulating the intracellular trafficking of APP.

The partitioning-defective (Par) polarity proteins are a group of evolutionarily conserved proteins that are essential for cell polarization from worms to mammals (6). In mammals, the Par proteins include Par1, 3, 4, 5 and 6. Of these, Par3 and Par6 form a complex with atypical PKC (aPKC) and Cdc42, which is commonly called the Par complex. The Par complex is essential for multiple cellular processes during animal development, including asymmetric cell division (7), epithelial morphogenesis (8,9), cell migration (10–15), axon specification (16–18) and dendritic spine formation (19–21). However, it is unknown whether the Par complex plays a role in brain aging and age-related neurodegeneration.

Increasing evidence points to a role for the Par polarity complex in vesicle trafficking. A genome-wide RNA interference screen revealed Par3, Par6, aPKC and Cdc42, all components of the Par polarity complex, as important regulators of endocytic trafficking (22). In addition, Par3, Par6 and aPKC interact with components of the exocyst complex (13,23,24). Furthermore, Cdc42, Par6 and aPKC regulate E-cadherin endocytosis, thereby maintaining epithelial polarity (25,26). Despite an emerging role for the Par complex in vesicle trafficking, the underlying molecular mechanism is still not well understood. Moreover, it is not known whether this complex is involved in trafficking of APP or its secretases.

Here we show that the Par complex regulates APP processing and trafficking. We found that in AD patients, the expression level of full length Par3 is significantly reduced. Knockdown of Par3 increases intracellular Aβ generation, while overexpression of Par3 promotes non-amyloidogenic APP processing. We further show that Par3 regulates APP trafficking by promoting its targeting to the recycling pathway, while knockdown of Par3 leads to late endosomal/lysosomal targeting of APP. Finally, we show that Par3 functions through disrupting the interaction between the endocytic adaptor Numb and APP. Together, our data show a novel role for Par3 in APP trafficking and Aβ generation.

Experimental Procedures

Plasmids and Reagents

All plasmids encoding full length or truncated versions of Par3b and Par3c, and Par3 shRNAs have been previously described (8,9,19,20). pcDNA3-APP was a generous gift from Dr. Sangram S. Sisodia (University of Chicago). For pcDNA3-APPmRFP, mRFP was inserted at the C-terminus of APP in the NotI site. GFP-Rab5 was generously provided by Dr. James Casanova (University of Virginia), GFP-Rab7 was a gift from Dr. John Brumell

(University of Toronto), and GFP-Rab11 was generously provided by Drs. Chan Choo Yap, Bettina Winckler (University of Virginia) and Ira Mellman (Genentech). For shRNA knockdown of Numb, the following oligonucleotides 5'-gatccccGATTGAAAGCTGAAAGGAAttcaagagaTTCCTTTCAGCTTTCAATCtttttggaaa-3' and 5'-agcttttccaaaaaGATTGAAAGCTGAAAGGAAtctcttgaaTTCCTTTCAGCTTTCAATCggg-3' were annealed and cloned into the pSUPER vector as previously described (27). GFP-Numb (p66 isoform) was generously provided by Dr. Ian Macara (Vanderbilt University). Neuro2a cells (N2a) stably expressing wild type human APP695 was a generous gift from Dr. Gopal Thinakaran (University of Chicago). Frozen human brain temporal lobe tissue was obtained from Sun Health Research Institute Brain and Body Donation Program of Sun City, AZ.

Primary hippocampal and cortical neurons and transfection

Hippocampal or cortical neuron cultures were prepared from embryonic day 18 Sprague-Dawley rats as described previously (27,28). Hippocampal neurons were transfected using either a CalPhos mammalian transfection kit (Clontech) or Effectene transfection reagent (Qiagen) at DIV 4–5 or DIV 10–11, respectively. Cortical neurons were infected with lentivirus at DIV 0.

Co-immunoprecipitation, Western Blotting and ELISA

For co-immunoprecipitation experiments, Neuro2a cells expressing different plasmid constructs or mouse brains were lysed on ice in buffer containing 25 mM Hepes, 150 mM NaCl, 10 mM $MgCl_2$, 1% Nonidet P-40, and 10 mM DTT and supplemented with protease inhibitor cocktail (Sigma-Aldrich), phosphatase inhibitor cocktail (Sigma-Aldrich), 10 mM β-glycerophosphate, and 10 mM NaF. Lysates were cleared by centrifugation at 13,000 *g* for 10 min at 4°C. Cleared lysates were incubated with anti-APP monoclonal antibody 6E10 (2 μg) for 1.5 h at 4°C followed by incubation with 20 μl of Dynabeads Protein G preblocked with 5% BSA in lysis buffer for another 3 hours. Beads were washed three times with lysis buffer. Bound proteins were eluted with 3× Laemmli sample buffer and subjected to SDS-PAGE and Western blot analysis.

For Western blot analysis, the primary antibodies used were mouse anti-APP antibody (1:2000, 6E10, Signet), mouse anti-APP antibody (1:1000, 22C11, Millipore), rabbit anti-APP antibody (1:8000, A8717, Sigma-Aldrich), rabbit anti-Par3 antibody (1:5000; a generous gift from Dr. Ian Macara), rabbit anti-BACE1 antibody (1:2000, D10E5, Cell Signaling), mouse anti-Presenilin-1 (1:1000, PS1-loop, Millipore), rabbit anti-Numb antibody (1:2000, Proteintech), mouse anti-GAPDH antibody (1:8000, 6C5, Millipore), and rabbit anti-GFP antibody (1:1000, A-11122, Life Technologies). The secondary antibodies used were Horseradish peroxidase-conjugated goat anti-mouse or rabbit antibody (1:5000 Jackson ImmunoResearch Laboratories, West Grove, PA). Proteins were visualized by enhanced chemiluminescence and imaged using a Syngene G:BOX iChemi XR system and GeneSnap software (Version 7.09.a; Syngene USA, Frederick, MD).

For ELISA measurements of Aβ40, primary cortical neurons were infected with different constructs at DIV0. Five days after infection, media supernatants were collected for

measurement of secreted Aβ40. Neurons were lysed for measurement of intracellular Aβ40. Aβ40 was measured using an ELISA kit obtained from Wako Chemicals (Cat. No. 294-62501) following the manufacturer's protocol.

Immunocytochemistry and immunohistochemistry

Hippocampal neurons or N2a cells were fixed in 4% paraformaldehyde (PFA) with 4% sucrose in PBS for 15 min at room temperature, then permeabilized with 0.2% Triton X-100 in PBS for 5 min at room temperature. Cells were blocked with 20% goat serum in PBS for 1 h at room temperature and then incubated with primary antibodies diluted in 5% goat serum in PBS for 1 h at room temperature or overnight at 4 °C. Primary antibodies used include 6E10 (1:100), TGN46 (rabbit polyclonal to TGN46, 1:800, Abcam) and LAMP1 (rabbit polyclonal to LAMP1, 1:500, Abcam). Following washes with PBS, Alexa Fluor 405, 488, or 594- conjugated secondary antibodies (Invitrogen) diluted in 5% goat serum were incubated with the neurons at room temperature for 1 h. Neurons were then washed with PBS and mounted using VECTASHIELD (Vector Laboratories, Burlingame, CA).

For APP surface or recycling immunostaining, hippocampal neurons were transfected with APP-RFP at DIV5. At DIV9, neurons were washed with PBS and live labeled with 6E10 diluted in Neurobasal media. For surface staining, neurons were live labeled at 20°C for 60 min, then fixed with 4% PFA with 4% sucrose and stained with Alexa Fluor 488- conjugated secondary antibody (29). For staining of recycled APP, neurons were live labeled with 6E10 for 30 min at 10°C and then incubated in 37°C for 1 hour. After PBS washes, neurons were blocked by HRP-conjugated secondary antibody diluted in Neurobasal media for 1 hour at 10°C and then incubated at 37 °C for another 1 hour. After 4% PFA fixation, neurons were stained with Alexa Fluor 488- conjugated secondary antibody. Control neurons were directly stained with secondary antibody after blocking without further incubation.

For immunostaining of internalized APP, N2a cells stably expressing WT APP695 were stained with 6E10 for 1 hour at 4 °C, and then incubated at 37°C for 20 or 60 min. Cells were fixed in 4% paraformaldehyde with 4% sucrose in PBS for 15 min at room temperature, and then blocked by HRP-conjugated secondary antibody for 1 hour at room temperature. After washing by PBS, cells were permeabilized with 0.2% Triton X-100 in PBS for 5 min at room temperature and then immunostained with the indicated primary or secondary antibodies.

Surface biotinylation

For surface biotinylation, N2a cells stably expressing WT APP695 were washed with PBS, then incubated in 1mM Sulfo-NHS-SS-Biotin (Pierce) in PBS for 1 hour in 4 °C. Unreacted ester was quenched in cold 50mM Tris-HCl for 10 min. To examine internalization, cells were surface biotinylated and then incubated at 37 °C for 1 hour. Cells were then treated with cleavage buffer [50mM glutathione(Sigma-Aldrich), 90mM NaCl, 1.25mM $CaCl_2$, 1.25mM $MgSO_4$, 0.2% BSA pH8.6] for 30 min at 4°C. For recycling, cells were surface biotinylated and incubated at 37°C to allow internalization. Surface biotin was cleaved as above and cells were returned to 37°C for another 30 min in serum free DMEM medium. Surface biotin was then cleaved again with the same cleavage buffer for another 30 min.

Cells were then lysed in cell lysis buffer (50mM Tris-HCl, pH7.5, 150mM NaCl, 2mM EDTA, 1% Triton X-100), containing protease inhibitor cocktail (Sigma-Aldrich). Lysates were incubated with NeutrAvidin-agarose beads (Pierce) in a rotary shaker for 3 hours at 4 °C. Beads were washed three times with cell lysis buffer and analyzed by SDS-PAGE followed by immunoblotting.

Image Acquisition and Quantification

Confocal images were obtained using an Olympus FV1000 confocal microscope with a 60 × water immersion objective (1.0 numerical aperture) with sequential-acquisition setting. Co-localization measurements were performed using NIH ImageJ.

Statistical analysis

All experiments were repeated at least three times. Unpaired Student's *t*-tests or One-Way ANOVA were used to calculate the p values. Error bars represent the S.E.M. of the samples.

Results

Loss of full length Par3 in human AD brains

A previous study found that Par3 and PKCζ, one of the two mammalian aPKCs, are among the top dysregulated genes in human AD samples (30). Thus, we hypothesized that the Par complex is involved in AD pathogenesis. To test this idea, we first examined Par3 protein expression levels in human AD patients. Previous studies show that the predominant isoform of Par3 in the brain is the full length, 180 KD isoform, with low levels of the C-terminally truncated 100 KD isoform, which lacks the region that binds many important partners including aPKC, Numb, TIAM1 and KIF3 (8,19,31–34). Consistent with this, we found that in healthy subjects, the major Par3 isoform expressed is the full length, 180KD isoform. In AD patients, there is a dramatic loss of full-length Par3 compared with age-matched healthy controls (Fig. 1a and b). These results suggest that the loss of full-length Par3 may be important in the AD pathogenic process.

Par3 regulates APP processing and Aβ generation

To test our hypothesis that loss of full length Par3 is important for AD progression, we first aimed to determine whether Par3 is involved in APP processing and Aβ generation. To examine the effects of Par3 on APP processing, we overexpressed or knocked down Par3 in Neuro2a (N2a) cells stably expressing wild type APP (35). Overexpression of Par3 increased the generation of C-terminal fragment α (CTFα), a cleavage product of α-secretase. By contrast, knockdown of Par3 significantly decreased the amount of CTFα (Fig. 2a and c). Total APP, BACE1 and PS1 levels were not significantly affected. Similar results were obtained when the γ-secretase inhibitor DAPT was present, indicating that the observed effect of Par3 is on α-secretase and not γ-secretase (Fig. S1a–c). Interestingly, under DAPT treatment in which CTFβ can be better resolved, we observed an increase in CTFβ/CTFα ratio in Par3 depleted cells, suggesting that Par3 depletion reduces α-cleavage while facilitating β-cleavage (Fig. S1b, d, e). To further test the effects of Par3 on APP processing, we examined the level of soluble APPα (sAPPα), another cleavage product of non-amyloidogenic α-secretase processing. Overexpression of Par3 caused a significant increase

in sAPPα in primary cortical neurons, while knockdown of Par3 caused a decrease in sAPPα (Fig. 2b and d). Taken together, these results suggest that Par3 promotes non-amyloidogenic APP processing.

Because APP processing affects Aβ generation, we next examined the effect of Par3 on Aβ generation. Par3 was either overexpressed or depleted in cortical neurons as described above. Both intracellular and secreted Aβ40 were then measured using an ELISA kit. Overexpression of Par3 reduced secreted Aβ40, but had no effect on intracellular Aβ40. Interestingly, knockdown of Par3 reduced secreted Aβ40 while increasing intracellular Aβ40 (Fig. 2e and f). Taken together, these results suggest that Par3 promotes non-amyloidogenic processing and loss of Par3 induces intracellular Aβ40 accumulation.

Par3 regulates APP trafficking

Since Par3 regulates APP processing, we wondered whether Par3 affects APP surface expression, as α-cleavage usually occurs on the cell surface (5). First, we live labeled for surface APP in hippocampal neurons using the 6E10 antibody to the extracellular domain of APP. As expected, Par3 overexpression increased surface APP, while depletion of Par3 significantly reduced surface APP (Fig. 3a and c). Similar effects were observed in N2a cells (data not shown). To confirm these results, we performed surface biotinylation in N2a cells stably expressing wild type APP (APPwt). Consistent with our results in hippocampal neurons, we observed a significant increase in surface APP upon Par3 overexpression, while Par3 depletion caused a significant decrease in surface APP (Fig. 3b and d).

The Par complex has been implicated in protein trafficking (13,22,23,25,26). Thus, we hypothesize that Par3 regulates APP processing and surface expression by modulating its trafficking. We used the biotinylation assay to examine APP endocytosis and recycling. To examine endocytosis, we surface biotinylated APPwt N2a cells at 4°C, then switched to 37°C to allow endocytosis. Remaining surface biotin was cleaved by glutathione. Cells were lysed and subjected to Western blot to determine the amount of internalized APP. The rate of internalization was not significantly altered (Fig. 4a and c). We then determined the rate of APP recycling. APPwt N2a cells were surface biotinylated and incubated at 37°C to allow internalization. They were then cooled to 4°C to stop membrane trafficking and the remaining surface biotin were cleaved. Cells were then returned to 37°C to allow for recycling and the newly inserted surface biotin was cleaved again. Cells were lysed and blotted for APP to determine the amount that remained intracellularly after recycling. Par3 overexpression caused a significant decrease in the amount of APP remaining intracellularly after recycling, which indicates Par3 promotes APP recycling to the cell surface (Fig. 4b and d). To confirm these results, we also examined APP recycling in hippocampal neurons. Live neurons were incubated with APP extracellular antibody. They were incubated at 37°C for 1 h to allow internalization. Neurons were cooled to stop internalization and the remaining surface APP was blocked by a cold secondary antibody. They were then returned to 37°C to allow recycling, and APP that had recycled to the cell surface were stained with a fluorescent secondary antibody. Consistent with our biotinylation results, neurons overexpressing Par3 showed significantly increased APP recycling while knockdown of Par3

decreased recycling (Fig. 4e and f). Taken together, our results show that Par3 promotes surface expression of APP by increasing its targeting to the recycling pathway.

To determine the fate of the internalized APP, we performed an antibody uptake assay in N2a cells stably expressing WT APP and co-immunostained internalized APP with markers of early endosomes (Fig. 5), late endosomes/lysosomes (Fig. 6) and recycling endosomes (Fig. 7). In Par3-depleted cells, internalized APP showed a significant increase in colocalization with Rab7, a marker for late endosomes/lysosomes, at 60 min after internalization (Fig. 6). By contrast, Par3-overexpressing cells showed a decrease in colocalization with Rab5, a marker for early endosomes (Fig. 5), with a concomitant increase in the colocalization of APP and Rab11, a marker for recycling endosomes, at 60 min after internalization (Fig. 7). This suggests that Par3 targets APP to the recycling pathway for re-insertion to the cell surface. In the absence of Par3, APP is targeted to the late endosome/lysosome pathway.

Par3 regulates APP trafficking through the endocytic adaptor protein Numb

The adaptor protein Numb mediates clathrin-dependent endocytosis of APP (36). In addition, Par3 interacts directly with Numb on its PTB domain (33), which is the same domain that mediates binding to membrane receptors such as integrins (33), Notch (37) and APP (38). To determine whether the effects of Par3 on APP trafficking and processing are mediated through Numb, we used shRNA to deplete endogenous Numb (Fig. 8a). Knockdown of Numb significantly increased CTFα indicating an increase in α-secretase processing, which phenocopies Par3 overexpression. Double knockdown of Numb and Par3 reversed the Par3 knockdown phenotype, suggesting that the effect of Par3 depletion is dependent on Numb (Fig. 8b and c). In addition, using live antibody labeling, we observed an increase in surface APP in hippocampal neurons depleted of Numb, and Numb knockdown was able to reverse the decrease in surface APP in Par3 knockdown neurons (Fig. 9a and b). To confirm these results, we performed surface biotinylation in N2a cells depleted of Numb and/or Par3. We found that Numb knockdown phenocopied Par3 overexpression and increased surface APP. In addition, Numb knockdown was able to reverse the decrease in surface APP in the Par3-depleted cells (Fig. 9c and d). Finally, using antibody feeding experiments as described above, we found that Numb depletion can reverse the late endosomal/lysosomal targeting of APP in Par3-depleted cells, as determined by the extent of colocalization of internalized APP with the lysosomal marker LAMP1 (Fig. 10). Together, these results suggest that the effects of Par3 on APP trafficking and processing are dependent on Numb.

To explore the mechanisms by which Par3 and Numb regulates APP trafficking, we examined the effects of Par3 on Numb-APP interaction. Since Par3 and APP bind to the same domain on Numb, we hypothesized that Par3 functions by interfering with the interaction between Numb and APP. We performed co-immunoprecipitation between APP and Numb with or without Par3. Indeed, APP-Numb interaction was significantly reduced when Par3 was overexpressed. By contrast, when Par3 was depleted, APP-Numb interaction was enhanced (Fig. 11). Taken together, our data suggest that Par3 regulates APP processing

and trafficking by interfering with the interaction between the endocytic adaptor protein Numb and APP.

Discussion

Intracellular trafficking properties of APP play an important role in how it is processed, which in turn determines the amount of Aβ generation. Because of the importance of this process in AD progression, there has been much research focused on elucidating the mechanisms of APP trafficking. In this study, we found that in AD patients, there is a dramatic loss of full length Par3 expression compared with age-matched healthy controls. We further found that Par3 regulates the trafficking of APP. Depletion of Par3 targets APP to late endosomes/lysosomes, while overexpression of Par3 targets APP to recycling endosomes for re-insertion to the cell surface. We could not detect any direct binding between Par3 and APP (data not shown); however, it is possible that Par3 is indirectly associated with APP through its binding partner Numb (33), which is known to bind the C-terminus of APP and mediates clathrin-dependent endocytosis of APP (36). Indeed, we found that the effects of Par3 are mediated through Numb. Par3 functions by interfering with the interaction between Numb and APP. In the absence of Par3, there is an increase in Numb-APP interaction leading to decreased surface APP and increased targeting of APP to late endosomal-lysosomal compartments.

Par3 is part of a conserved protein complex that regulates cell polarity from worms to mammals. While polarity establishment is essential for all stages of animal development, it is interesting to note that dysregulation of polarity signaling appears to be common in different aging processes and age-related diseases, such as stem cell aging and cancer (39–44). Here we show that Alzheimer's disease, the most common age-related neurodegeneration, is characterized by the loss of full length Par3, which indicates that dysregulation of polarity may be a common feature for many different age-related diseases.

Interestingly, Numb has been shown to regulate APP trafficking in an isoform-dependent manner (36). It has been shown that the short PTB isoforms of Numb promotes APP accumulation in the early and recycling endosome compartments, while the long PTB isoforms of Numb promotes the late endosome/lysosome targeting of APP. It has been shown that the long PTB isoforms are predominantly expressed under physiological conditions (36). In this study, we have used the p66 isoform which contains the long PTB domain. Further, we observed increased targeting of APP to late endosomes/lysosomes which is consistent with increase interaction between long PTB Numb and APP (36). It will be interesting to determine whether Par3 has differential effects on the short and long PTB isoforms of Numb and how this might be regulated during AD progression.

Remarkably, loss of Par3 leads to an accumulation of intracellular Aβ40 but a decrease in secreted Aβ40. It is known that during AD pathogenesis, intracellular Aβ accumulates before the deposition of extracellular Aβ plaques (45–50). In addition, a number of studies suggest that intracellular Aβ may be the major toxic form that is responsible for neurodegeneration (51–55). Lysosomes are shown to be an important site for Aβ generation (56). Furthermore, it has been reported that the intracellular Aβ accumulate in lysosomal compartments in the

AD brain (57,58). Consistent with these studies, we found that Par3 depletion causes APP to target to the lysosomes and increases intracellular Aβ40. A recent study shows that autophagy mediates the secretion of Aβ into the extracellular space. In the absence of autophagy, intracellular Aβ rises while extracellular Aβ deposits decrease (59), a phenotype reminiscent of what we observed in Par3-depleted neurons. It would be of great interest to examine whether Par3 is involved in autophagic processes.

In summary, our studies identified a novel role for the cell polarity regulator Par3 in APP processing and trafficking. We further identified a mechanism for Par3 in APP trafficking through interfering with Numb-APP interaction. Together, our results suggest a potential involvement of Par polarity proteins, which are central regulators of various developmental processes, in Alzheimer's disease pathogenesis. Further studies are necessary to elucidate the role of this interesting group of proteins in neurodegeneration.

Supplementary Material

Refer to Web version on PubMed Central for supplementary material.

Acknowledgments

We would like to thank Dr. Gopal Thinakaran (University of Chicago) for APP stable cell lines, Dr. Sangram S. Sisodia (University of Chicago) for WT APP695 plasmid, Drs. John Brumell (University of Toronto), Ira Mellman (Genentech), James Casanova, Chan Choo Yap and Bettina Winckler (University of Virginia) for different Rab plasmids. We thank Laura Bernard for technical assistance with the preparation of neuronal cultures. We would also like to thank members of the Zhang laboratory for critical reading of the manuscript. We are grateful to the Sun Health Research Institute Brain and Body Donation Program of Sun City, Arizona for the provision for human brain tissue. The Banner Sun Health Research Institute Brain and Body Donation Program is supported by the National Institute of Neurological Disorders and Stroke (U24 NS072026 National Brain and Tissue Resource for Parkinson's Disease and Related Disorders), the National Institute on Aging (P30 AG19610 Arizona Alzheimer's Disease Core Center), the Arizona Department of Health Services (contract 211002, Arizona Alzheimer's Research Center), the Arizona Biomedical Research Commission (contracts 4001, 0011, 05-901 and 1001 to the Arizona Parkinson's Disease Consortium) and the Michael J. Fox Foundation for Parkinson's Research. This work was supported by National Institutes of Health grants NS065183, NS089578 and startup fund from Rutgers Robert Wood Johnson Medical School.

References

1. Claeysen S, Cochet M, Donneger R, Dumuis A, Bockaert J, Giannoni P. Alzheimer culprits: cellular crossroads and interplay. Cell Signal. 2012; 24:1831–1840. [PubMed: 22627093]
2. Rajendran L, Annaert W. Membrane trafficking pathways in Alzheimer's disease. Traffic. 2012; 13:759–770. [PubMed: 22269004]
3. Tan J, Evin G. Beta-site APP-cleaving enzyme 1 trafficking and Alzheimer's disease pathogenesis. J Neurochem. 2012; 120:869–880. [PubMed: 22171895]
4. Pasternak SH, Bagshaw RD, Guiral M, Zhang S, Ackerley CA, Pak BJ, Callahan JW, Mahuran DJ. Presenilin-1, nicastrin, amyloid precursor protein, and gamma-secretase activity are co-localized in the lysosomal membrane. J Biol Chem. 2003; 278:26687–26694. [PubMed: 12736250]
5. Haass C, Kaether C, Thinakaran G, Sisodia S. Trafficking and proteolytic processing of APP. Cold Spring Harb Perspect Med. 2012; 2:a006270. [PubMed: 22553493]
6. Goldstein B, Macara IG. The PAR proteins: fundamental players in animal cell polarization. Dev Cell. 2007; 13:609–622. [PubMed: 17981131]
7. Goulas S, Conder R, Knoblich JA. The Par complex and integrins direct asymmetric cell division in adult intestinal stem cells. Cell Stem Cell. 2012; 11:529–540. [PubMed: 23040479]

8. Chen X, Macara IG. Par-3 controls tight junction assembly through the Rac exchange factor Tiam1. Nat Cell Biol. 2005; 7:262–269. [PubMed: 15723052]
9. McCaffrey LM, Macara IG. The Par3/aPKC interaction is essential for end bud remodeling and progenitor differentiation during mammary gland morphogenesis. Genes Dev. 2009; 23:1450–1460. [PubMed: 19528321]
10. Wang HR, Zhang Y, Ozdamar B, Ogunjimi AA, Alexandrova E, Thomsen GH, Wrana JL. Regulation of cell polarity and protrusion formation by targeting RhoA for degradation. Science. 2003; 302:1775–1779. [PubMed: 14657501]
11. Pegtel DM, Ellenbroek SI, Mertens AE, van der Kammen RA, de Rooij J, Collard JG. The Par-Tiam1 complex controls persistent migration by stabilizing microtubule-dependent front-rear polarity. Curr Biol. 2007; 17:1623–1634. [PubMed: 17825562]
12. Hidalgo-Carcedo C, Hooper S, Chaudhry SI, Williamson P, Harrington K, Leitinger B, Sahai E. Collective cell migration requires suppression of actomyosin at cell-cell contacts mediated by DDR1 and the cell polarity regulators Par3 and Par6. Nat Cell Biol. 2011; 13:49–58. [PubMed: 21170030]
13. Das A, Gajendra S, Falenta K, Oudin MJ, Peschard P, Feng S, Wu B, Marshall CJ, Doherty P, Guo W, Lalli G. RalA promotes a direct exocyst-Par6 interaction to regulate polarity in neuronal development. J Cell Sci. 2014; 127:686–699. [PubMed: 24284074]
14. Solecki DJ, Model L, Gaetz J, Kapoor TM, Hatten ME. Par6alpha signaling controls glial-guided neuronal migration. Nat Neurosci. 2004; 7:1195–1203. [PubMed: 15475953]
15. Famulski JK, Trivedi N, Howell D, Yang Y, Tong Y, Gilbertson R, Solecki DJ. Siah regulation of Pard3A controls neuronal cell adhesion during germinal zone exit. Science. 2010; 330:1834–1838. [PubMed: 21109632]
16. Shi SH, Jan LY, Jan YN. Hippocampal neuronal polarity specified by spatially localized mPar3/mPar6 and PI 3-kinase activity. Cell. 2003; 112:63–75. [PubMed: 12526794]
17. Chen S, Chen J, Shi H, Wei M, Castaneda-Castellanos DR, Bultje RS, Pei X, Kriegstein AR, Zhang M, Shi SH. Regulation of microtubule stability and organization by mammalian Par3 in specifying neuronal polarity. Dev Cell. 2013; 24:26–40. [PubMed: 23273878]
18. Hengst U, Deglincerti A, Kim HJ, Jeon NL, Jaffrey SR. Axonal elongation triggered by stimulus-induced local translation of a polarity complex protein. Nat Cell Biol. 2009; 11:1024–1030. [PubMed: 19620967]
19. Zhang H, Macara IG. The polarity protein PAR-3 and TIAM1 cooperate in dendritic spine morphogenesis. Nat Cell Biol. 2006; 8:227–237. [PubMed: 16474385]
20. Zhang H, Macara IG. The PAR-6 polarity protein regulates dendritic spine morphogenesis through p190 RhoGAP and the Rho GTPase. Dev Cell. 2008; 14:216–226. [PubMed: 18267090]
21. Duman JG, Tzeng CP, Tu YK, Munjal T, Schwechter B, Ho TS, Tolias KF. The adhesion-GPCR BAI1 regulates synaptogenesis by controlling the recruitment of the Par3/Tiam1 polarity complex to synaptic sites. J Neurosci. 2013; 33:6964–6978. [PubMed: 23595754]
22. Balklava Z, Pant S, Fares H, Grant BD. Genome-wide analysis identifies a general requirement for polarity proteins in endocytic traffic. Nat Cell Biol. 2007; 9:1066–1073. [PubMed: 17704769]
23. Lalli G. RalA and the exocyst complex influence neuronal polarity through PAR-3 and aPKC. J Cell Sci. 2009; 122:1499–1506. [PubMed: 19383721]
24. Zuo X, Guo W, Lipschutz JH. The exocyst protein Sec10 is necessary for primary ciliogenesis and cystogenesis in vitro. Mol Biol Cell. 2009; 20:2522–2529. [PubMed: 19297529]
25. Georgiou M, Marinari E, Burden J, Baum B. Cdc42, Par6, and aPKC regulate Arp2/3-mediated endocytosis to control local adherens junction stability. Curr Biol. 2008; 18:1631–1638. [PubMed: 18976918]
26. Leibfried A, Fricke R, Morgan MJ, Bogdan S, Bellaiche Y. Drosophila Cip4 and WASp define a branch of the Cdc42-Par6-aPKC pathway regulating E-cadherin endocytosis. Curr Biol. 2008; 18:1639–1648. [PubMed: 18976911]
27. Wu Q, DiBona VL, Bernard LP, Zhang H. The polarity protein partitioning-defective 1 (PAR-1) regulates dendritic spine morphogenesis through phosphorylating postsynaptic density protein 95 (PSD-95). J Biol Chem. 2012; 287:30781–30788. [PubMed: 22807451]

28. Bernard LP, Zhang H. MARK/Par1 Kinase Is Activated Downstream of NMDA Receptors through a PKA-Dependent Mechanism. PLoS One. 2015; 10:e0124816. [PubMed: 25932647]
29. Carrodus NL, Teng KS, Munro KM, Kennedy MJ, Gunnersen JM. Differential labeling of cell-surface and internalized proteins after antibody feeding of live cultured neurons. J Vis Exp. 2014:e51139. [PubMed: 24561550]
30. Tan MG, Chua WT, Esiri MM, Smith AD, Vinters HV, Lai MK. Genome wide profiling of altered gene expression in the neocortex of Alzheimer's disease. J Neurosci Res. 2010; 88:1157–1169. [PubMed: 19937809]
31. Joberty G, Petersen C, Gao L, Macara IG. The cell-polarity protein Par6 links Par3 and atypical protein kinase C to Cdc42. Nat Cell Biol. 2000; 2:531–539. [PubMed: 10934474]
32. Lin D, Edwards AS, Fawcett JP, Mbamalu G, Scott JD, Pawson T. A mammalian PAR-3-PAR-6 complex implicated in Cdc42/Rac1 and aPKC signalling and cell polarity. Nat Cell Biol. 2000; 2:540–547. [PubMed: 10934475]
33. Nishimura T, Kaibuchi K. Numb controls integrin endocytosis for directional cell migration with aPKC and PAR-3. Dev Cell. 2007; 13:15–28. [PubMed: 17609107]
34. Nishimura T, Kato K, Yamaguchi T, Fukata Y, Ohno S, Kaibuchi K. Role of the PAR-3-KIF3 complex in the establishment of neuronal polarity. Nat Cell Biol. 2004; 6:328–334. [PubMed: 15048131]
35. Thinakaran G, Teplow DB, Siman R, Greenberg B, Sisodia SS. Metabolism of the "Swedish" amyloid precursor protein variant in neuro2a (N2a) cells. Evidence that cleavage at the "beta-secretase" site occurs in the golgi apparatus. J Biol Chem. 1996; 271:9390–9397. [PubMed: 8621605]
36. Kyriazis GA, Wei Z, Vandermey M, Jo DG, Xin O, Mattson MP, Chan SL. Numb endocytic adapter proteins regulate the transport and processing of the amyloid precursor protein in an isoform-dependent manner: implications for Alzheimer disease pathogenesis. J Biol Chem. 2008; 283:25492–25502. [PubMed: 18599481]
37. Guo M, Jan LY, Jan YN. Control of daughter cell fates during asymmetric division: interaction of Numb and Notch. Neuron. 1996; 17:27–41. [PubMed: 8755476]
38. Roncarati R, Sestan N, Scheinfeld MH, Berechid BE, Lopez PA, Meucci O, McGlade JC, Rakic P, D'Adamio L. The gamma-secretase-generated intracellular domain of beta-amyloid precursor protein binds Numb and inhibits Notch signaling. Proc Natl Acad Sci U S A. 2002; 99:7102–7107. [PubMed: 12011466]
39. Shcheprova Z, Baldi S, Frei SB, Gonnet G, Barral Y. A mechanism for asymmetric segregation of age during yeast budding. Nature. 2008; 454:728–734. [PubMed: 18660802]
40. Geiger H, de Haan G, Florian MC. The ageing haematopoietic stem cell compartment. Nat Rev Immunol. 2013; 13:376–389. [PubMed: 23584423]
41. Florian MC, Dorr K, Niebel A, Daria D, Schrezenmeier H, Rojewski M, Filippi MD, Hasenberg A, Gunzer M, Scharffetter-Kochanek K, Zheng Y, Geiger H. Cdc42 activity regulates hematopoietic stem cell aging and rejuvenation. Cell Stem Cell. 2012; 10:520–530. [PubMed: 22560076]
42. McCaffrey LM, Montalbano J, Mihai C, Macara IG. Loss of the Par3 polarity protein promotes breast tumorigenesis and metastasis. Cancer Cell. 2012; 22:601–614. [PubMed: 23153534]
43. Iden S, van Riel WE, Schafer R, Song JY, Hirose T, Ohno S, Collard JG. Tumor type-dependent function of the par3 polarity protein in skin tumorigenesis. Cancer Cell. 2012; 22:389–403. [PubMed: 22975380]
44. Xue B, Krishnamurthy K, Allred DC, Muthuswamy SK. Loss of Par3 promotes breast cancer metastasis by compromising cell-cell cohesion. Nat Cell Biol. 2013; 15:189–200. [PubMed: 23263278]
45. Chui DH, Tanahashi H, Ozawa K, Ikeda S, Checler F, Ueda O, Suzuki H, Araki W, Inoue H, Shirotani K, Takahashi K, Gallyas F, Tabira T. Transgenic mice with Alzheimer presenilin 1 mutations show accelerated neurodegeneration without amyloid plaque formation. Nat Med. 1999; 5:560–564. [PubMed: 10229234]
46. Gouras GK, Tsai J, Naslund J, Vincent B, Edgar M, Checler F, Greenfield JP, Haroutunian V, Buxbaum JD, Xu H, Greengard P, Relkin NR. Intraneuronal Abeta42 accumulation in human brain. Am J Pathol. 2000; 156:15–20. [PubMed: 10623648]

47. Oddo S, Caccamo A, Shepherd JD, Murphy MP, Golde TE, Kayed R, Metherate R, Mattson MP, Akbari Y, LaFerla FM. Triple-transgenic model of Alzheimer's disease with plaques and tangles: intracellular Abeta and synaptic dysfunction. Neuron. 2003; 39:409–421. [PubMed: 12895417]

48. Oakley H, Cole SL, Logan S, Maus E, Shao P, Craft J, Guillozet-Bongaarts A, Ohno M, Disterhoft J, Van Eldik L, Berry R, Vassar R. Intraneuronal beta-amyloid aggregates, neurodegeneration, and neuron loss in transgenic mice with five familial Alzheimer's disease mutations: potential factors in amyloid plaque formation. J Neurosci. 2006; 26:10129–10140. [PubMed: 17021169]

49. Knobloch M, Konietzko U, Krebs DC, Nitsch RM. Intracellular Abeta and cognitive deficits precede beta-amyloid deposition in transgenic arcAbeta mice. Neurobiol Aging. 2007; 28:1297–1306. [PubMed: 16876915]

50. Youmans KL, Tai LM, Kanekiyo T, Stine WB Jr, Michon SC, Nwabuisi-Heath E, Manelli AM, Fu Y, Riordan S, Eimer WA, Binder L, Bu G, Yu C, Hartley DM, LaDu MJ. Intraneuronal Abeta detection in 5xFAD mice by a new Abeta-specific antibody. Mol Neurodegener. 2012; 7:8. [PubMed: 22423893]

51. Zhang Y, McLaughlin R, Goodyer C, LeBlanc A. Selective cytotoxicity of intracellular amyloid beta peptide1–42 through p53 and Bax in cultured primary human neurons. J Cell Biol. 2002; 156:519–529. [PubMed: 11815632]

52. Soejima N, Ohyagi Y, Nakamura N, Himeno E, Iinuma KM, Sakae N, Yamasaki R, Tabira T, Murakami K, Irie K, Kinoshita N, LaFerla FM, Kiyohara Y, Iwaki T, Kira J. Intracellular accumulation of toxic turn amyloid-beta is associated with endoplasmic reticulum stress in Alzheimer's disease. Curr Alzheimer Res. 2013; 10:11–20. [PubMed: 22950910]

53. Magrane J, Rosen KM, Smith RC, Walsh K, Gouras GK, Querfurth HW. Intraneuronal beta-amyloid expression downregulates the Akt survival pathway and blunts the stress response. J Neurosci. 2005; 25:10960–10969. [PubMed: 16306409]

54. Pigino G, Morfini G, Atagi Y, Deshpande A, Yu C, Jungbauer L, LaDu M, Busciglio J, Brady S. Disruption of fast axonal transport is a pathogenic mechanism for intraneuronal amyloid beta. Proc Natl Acad Sci U S A. 2009; 106:5907–5912. [PubMed: 19321417]

55. Tampellini D, Rahman N, Gallo EF, Huang Z, Dumont M, Capetillo-Zarate E, Ma T, Zheng R, Lu B, Nanus DM, Lin MT, Gouras GK. Synaptic activity reduces intraneuronal Abeta, promotes APP transport to synapses, and protects against Abeta-related synaptic alterations. J Neurosci. 2009; 29:9704–9713. [PubMed: 19657023]

56. Tam JH, Seah C, Pasternak SH. The Amyloid Precursor Protein is rapidly transported from the Golgi apparatus to the lysosome and where it is processed into beta-amyloid. Mol Brain. 2014; 7:54. [PubMed: 25085554]

57. Yu WH, Cuervo AM, Kumar A, Peterhoff CM, Schmidt SD, Lee JH, Mohan PS, Mercken M, Farmery MR, Tjernberg LO, Jiang Y, Duff K, Uchiyama Y, Naslund J, Mathews PM, Cataldo AM, Nixon RA. Macroautophagy--a novel Beta-amyloid peptide-generating pathway activated in Alzheimer's disease. J Cell Biol. 2005; 171:87–98. [PubMed: 16203860]

58. Langui D, Girardot N, El Hachimi KH, Allinquant B, Blanchard V, Pradier L, Duyckaerts C. Subcellular topography of neuronal Abeta peptide in APPxPS1 transgenic mice. Am J Pathol. 2004; 165:1465–1477. [PubMed: 15509518]

59. Nilsson P, Loganathan K, Sekiguchi M, Matsuba Y, Hui K, Tsubuki S, Tanaka M, Iwata N, Saito T, Saido TC. Abeta secretion and plaque formation depend on autophagy. Cell Rep. 2013; 5:61–69. [PubMed: 24095740]

Highlights

- Alzheimer's disease patients show a loss of full length Par3 in the brain.
- Loss of Par3 reduces α-cleavage of APP and increases intracellular Aβ40.
- Par3 promotes APP recycling to the cell surface.
- Loss of Par3 increases late endosome/lysosome targeting of APP.
- Par3 functions through interfering with the interaction between APP and Numb.

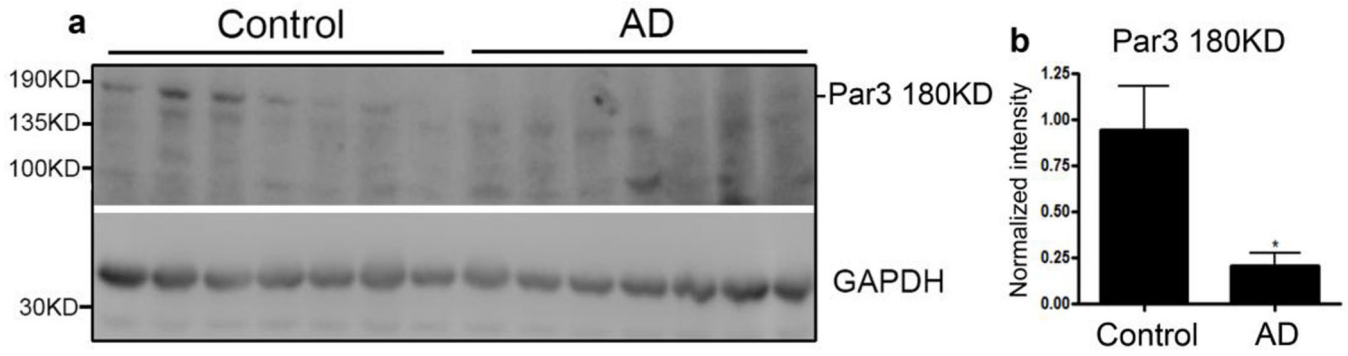

Figure 1. Loss of full length Par3 in human AD brains

(a) Lysates from the temporal lobes of AD patients or healthy age-matched controls were analyzed by Western blotting.

(b) Quantification of levels of the full length, 180KD isoform of Par3. Data were expressed as Mean ± SEM with Student's t test: N=7; *p<0.05.

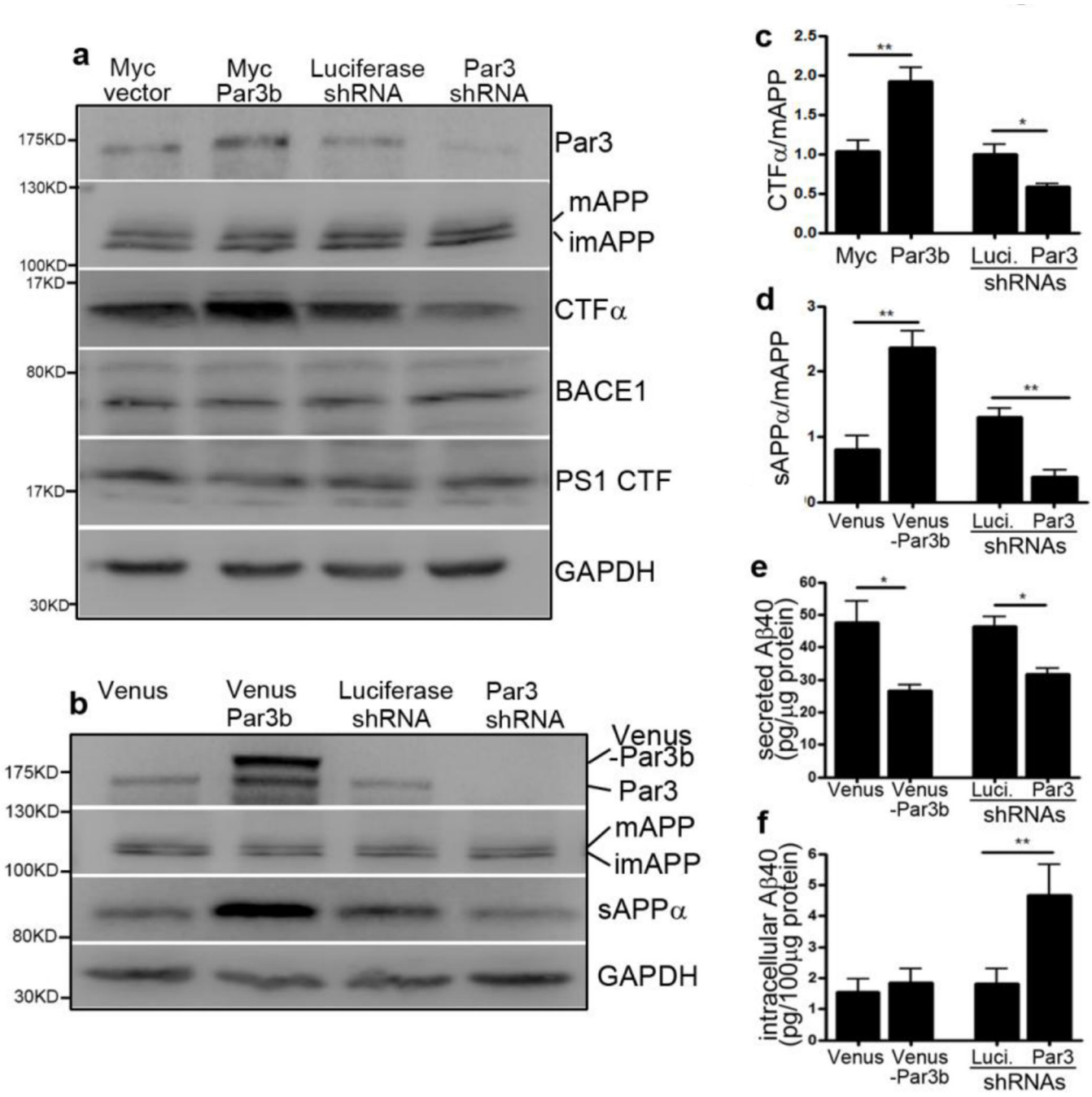

Figure 2. Par3 regulate APP processing and Aβ generation

(a) N2a cells stably expressing WT APP (APPwt) were transfected with plasmids encoding myc tag vector control (Myc vector), myc-Par3b, luciferase shRNA or Par3 shRNA, respectively. 72 h after transfection, cell were lysed, total protein was extracted and subjected to Western blot analysis with the indicated antibodies. APP was probed with A8717 antibody. mAPP: mature APP; imAPP, immature APP. (b) Cortical neurons were infected with lentivirus expressing Venus vector control (Venus), Venus-Par3b, Luciferase shRNA or Par3 shRNA. Five days after infection, media supernatants were collected for

detecting sAPPα using the 6E10 antibody. Neurons were lysed, total protein was extracted and subjected to Western blot analysis with the indicated antibodies. (c) Quantification of C-terminal fragment α of APP (CTFα) normalized to mature APP, n=3. (d) Quantification of soluble APPα (sAPPα) normalized to mature APP, n=3. (e, f) Cortical neurons were infected with lentivirus expressing the indicated constructs. ELISA assay was used to measure (e) secreted Aβ40, or (f) intracellular Aβ40 normalized to total protein levels, n=9. Data were expressed as Mean ± SEM with Student's t test: *p<0.05; **p<0.01.

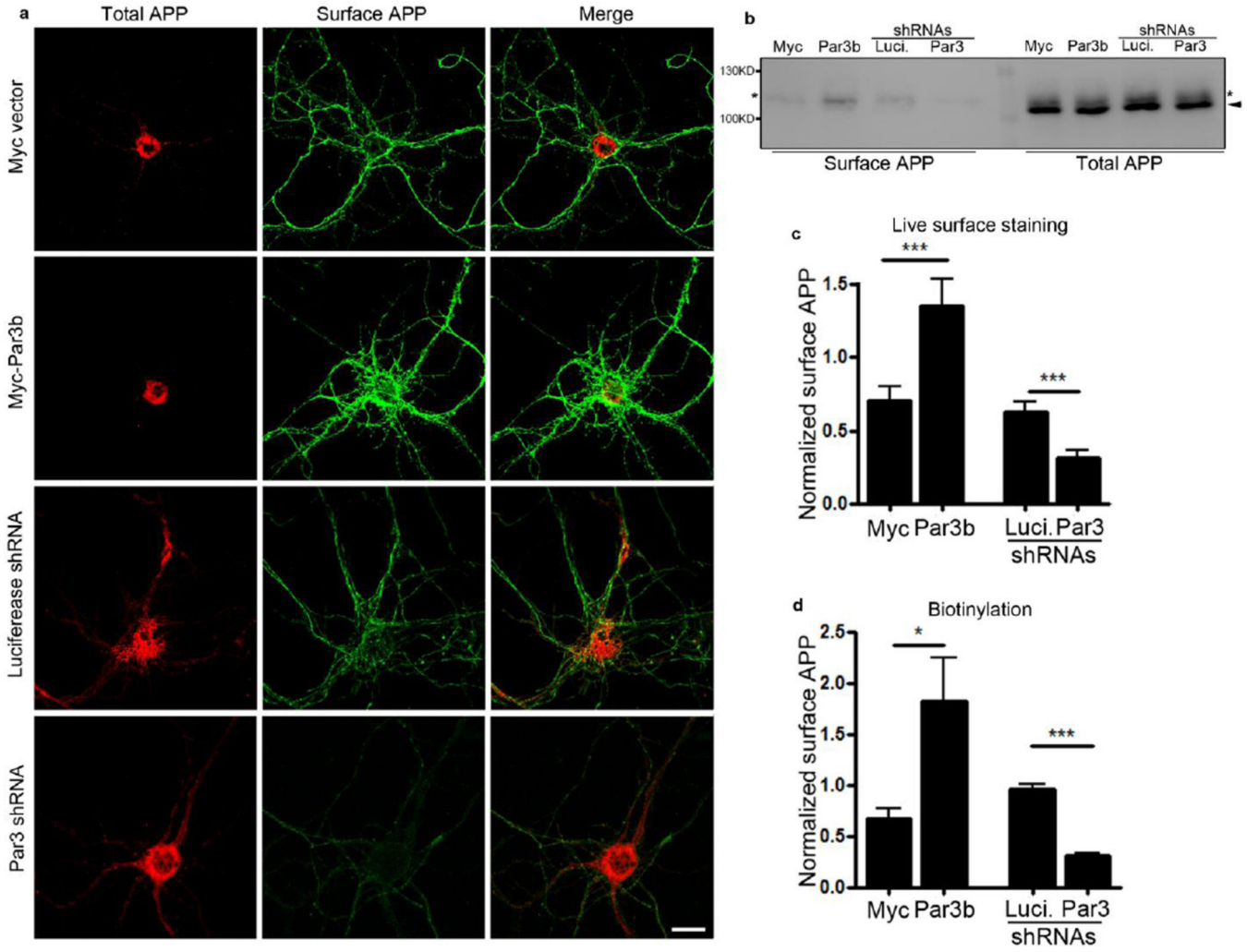

Figure 3. Depletion of Par3 decreases surface APP

(a) Hippocampal neurons were transfected with APP-RFP together with the indicated constructs and live labeled for surface APP using 6E10 antibody (green). Scale bar: 10 μm.

(b) APPwt N2a cells were transfected with the indicated constructs and surface biotinylated to measure surface APP levels. Biotinylated surface proteins were analyzed by Western blotting to reveal surface APP levels. Asterisks indicate mature APP, arrowhead indicates immature APP.

(c) Quantification of surface APP fluorescent intensity normalized to APP-RFP intensity, n=5–10, *** $p<0.001$.

(d) Quantification of surface APP normalized to mature APP, n=4. Data were expressed as Mean ± SEM with Student's t test: *$p<0.05$; ** $p<0.01$; *** $p<0.001$.

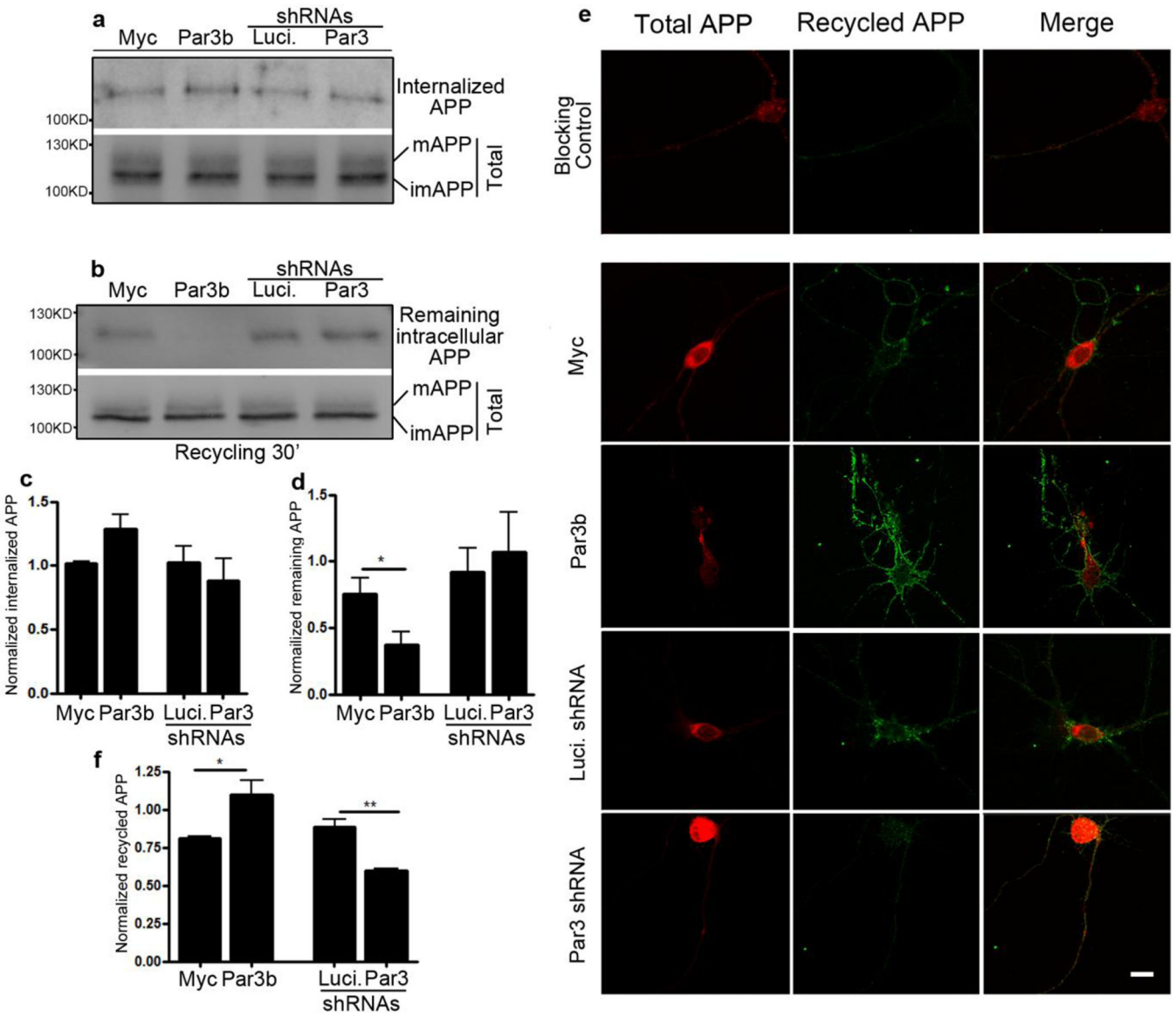

Figure 4. Par3 regulates APP trafficking

(a, b) APPwt N2a cells were transfected with the indicated constructs and biotinylation assays of (a) APP internalization or (b) APP recycling were performed (see Experimental Procedures). mAPP, mature APP; imAPP, immature APP. (c) Quantification of internalized APP normalized to mature APP, n=5. (d) Quantification of APP that remains intracellular after recycling, normalized to mature APP, n=4. (e) Hippocampal neurons were transfected with APP-RFP and the indicated constructs and live labeled with APP antibody. APP that has recycled to the cell surface was immunostained (green, see Experimental Procedures for details). (f) Quantification of the fluorescent intensity of APP that has recycled to the cell surface, normalized to the intensity of APP-RFP, n=8–12. Data were expressed as Mean ± SEM with Student's t test: *$p<0.05$; ** $p<0.01$. Scale bar: 10μm.

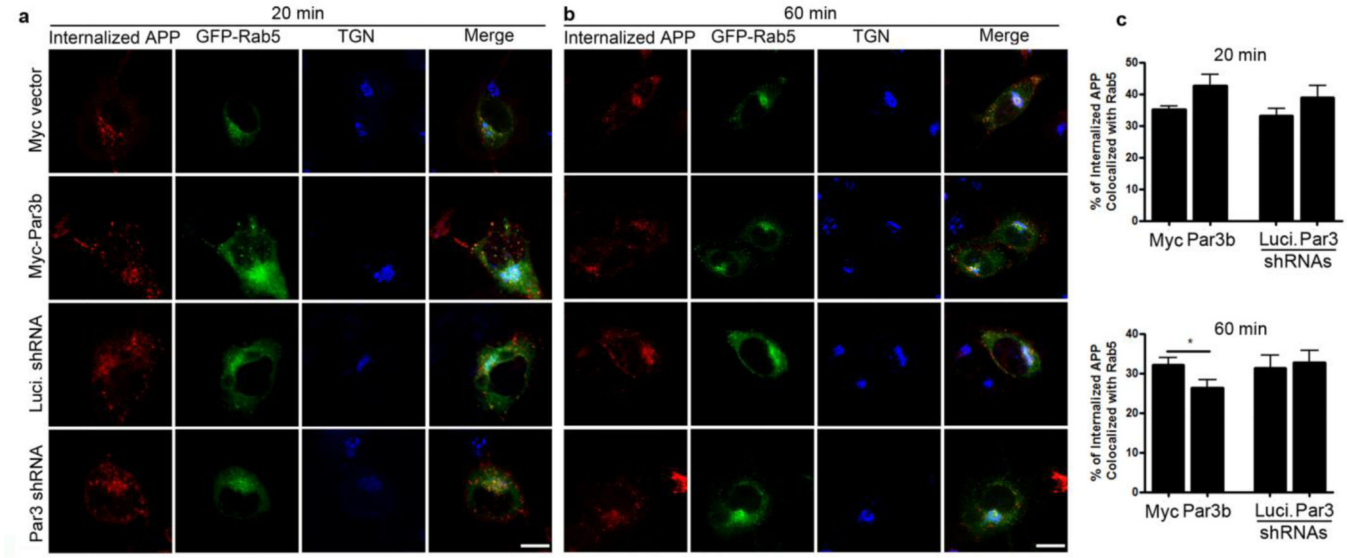

Figure 5. Colocalization of internalized APP with the early endosomal marker Rab5

APPwt N2a cells were transfected with indicated constructs together with GFP-Rab5 (green) and then live labeled with APP 6E10 antibody. Cells were fixed at 20 (a) or 60 min (b) after internalization and immunostained for internalized APP (red) and TGN46 (blue). (c) Quantification of colocalization between internalized APP and Rab5. Data were expressed as Mean ± SEM with Student's t test, *$p<0.05$. n=10–15. Scale bar: 10μm.

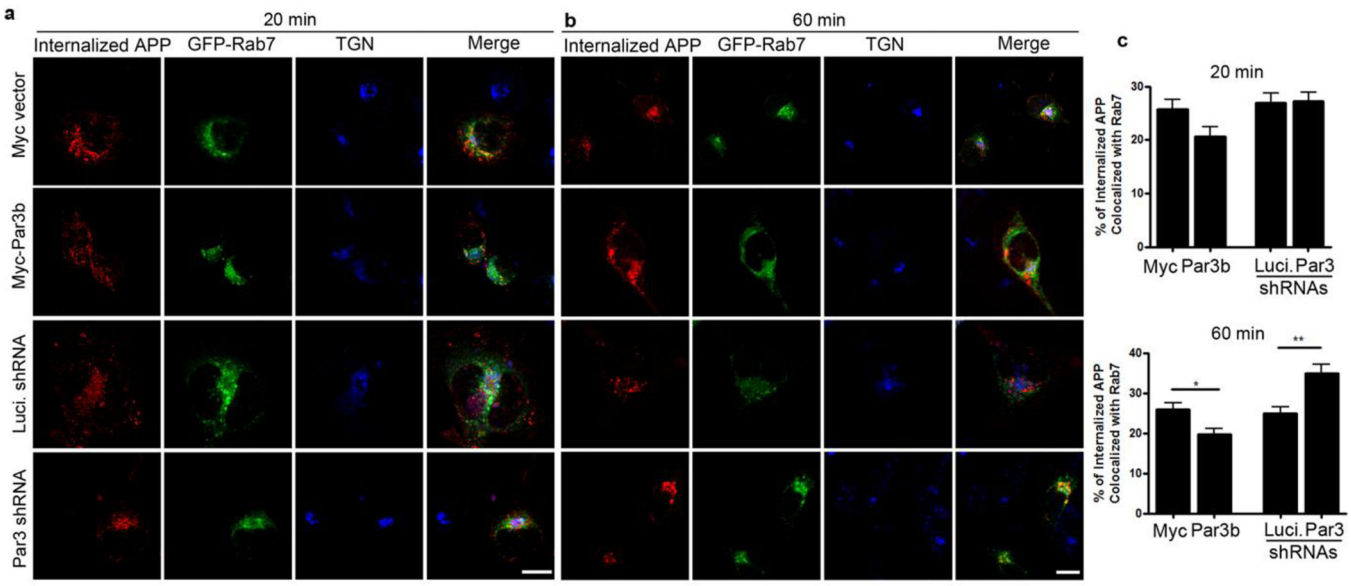

Figure 6. Colocalization of internalized APP with the late endosomal/lysosomal marker Rab7

APPwt N2a cells were transfected with indicated constructs together with GFP-Rab7 (green) and then live labeled with APP 6E10 antibody. Cells were fixed at 20 (a) or 60 min (b) after internalization and immunostained for internalized APP (red) and TGN46 (blue). (c) Quantification of colocalization between internalized APP and Rab7. Data were expressed as Mean ± SEM with Student's t test, *$p<0.05$; ** $p<0.01$. n=10–15. Scale bar: 10μm.

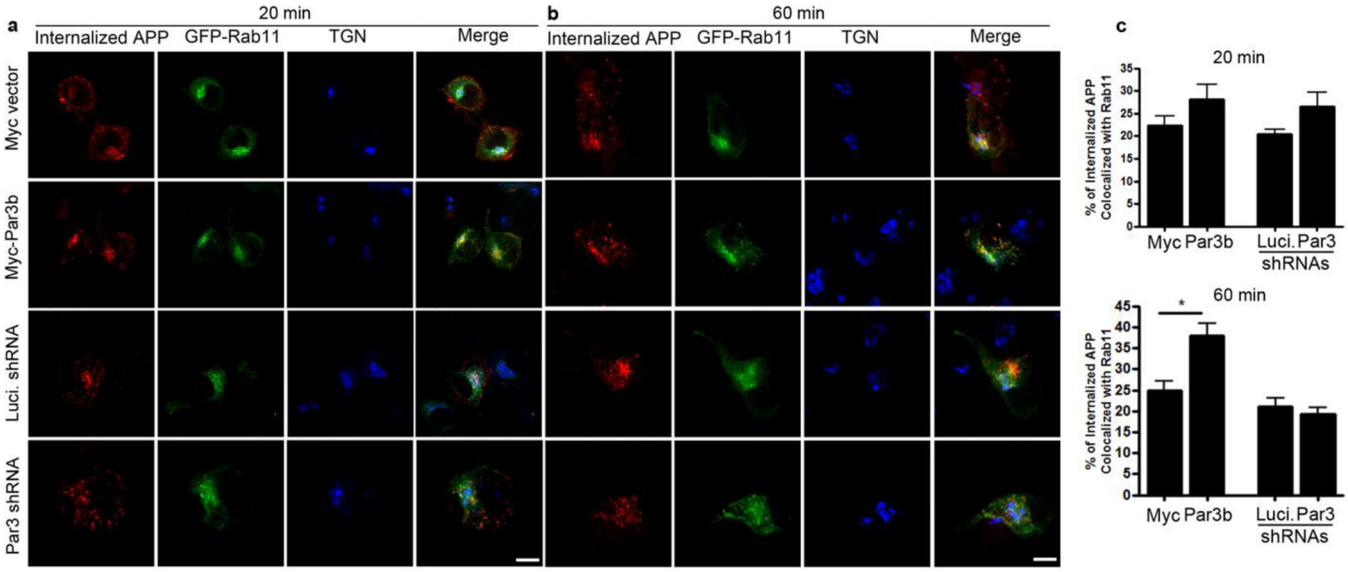

Figure 7. Colocalization of internalized APP with the recycling endosomal marker Rab11

APPwt N2a cells were transfected with indicated constructs together with GFP-Rab11 (green) and then live labeled with APP 6E10 antibody. Cells were fixed at 20 (a) or 60 min (b) after internalization and immunostained for internalized APP (red) and TGN46 (blue). (c) Quantification of colocalization between internalized APP and Rab11. Data were expressed as Mean ± SEM with Student's t test, *$p<0.05$. n=10–15. Scale bar: 10μm.

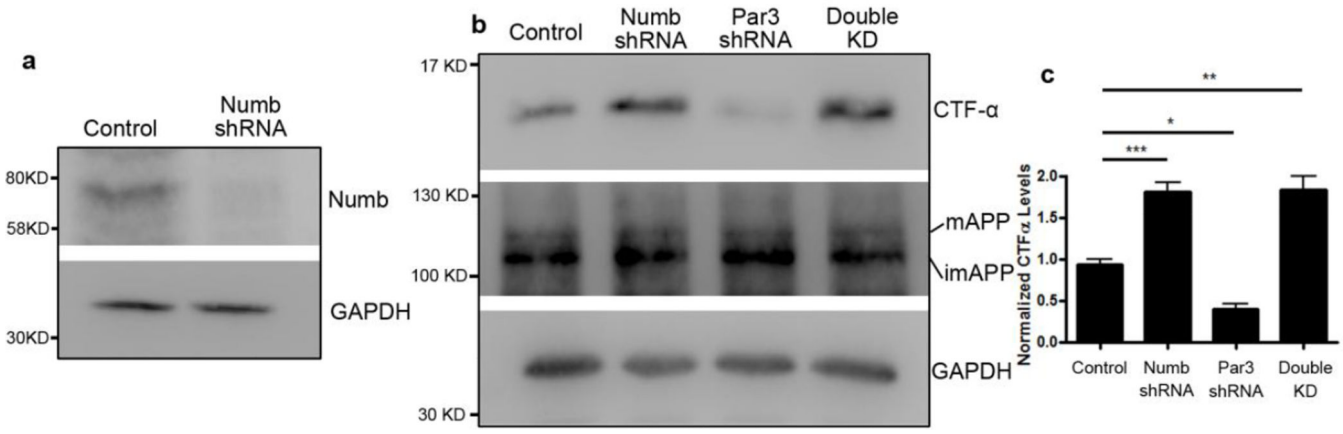

Figure 8. Knockdown of Numb rescues the decrease in CTFα in Par3-depleted cells

(a) Knockdown of Numb in N2a cells. N2a cells were transfected with pSUPER constructs encoding either an shRNA targeting luciferase (control) or Numb. 72 hours after transfection, cells were lysed and subjected to Western blot using the indicated antibodies.

(b) N2a cells stably expressing WT APP (APPwt) were transfected with plasmids encoding shRNA targeting luciferase (Control), Numb shRNA, Par3 shRNA, or both Numb and Par3 shRNAs [Double knockdown (KD)], respectively. 72 h after transfection, cell were lysed, total protein was extracted and subjected to Western blot analysis.

(c) Quantification of blots in b. Data were expressed as Mean ± SEM with Student's t test: *p<0.05; ** p<0.01, ***p<0.001, n=3.

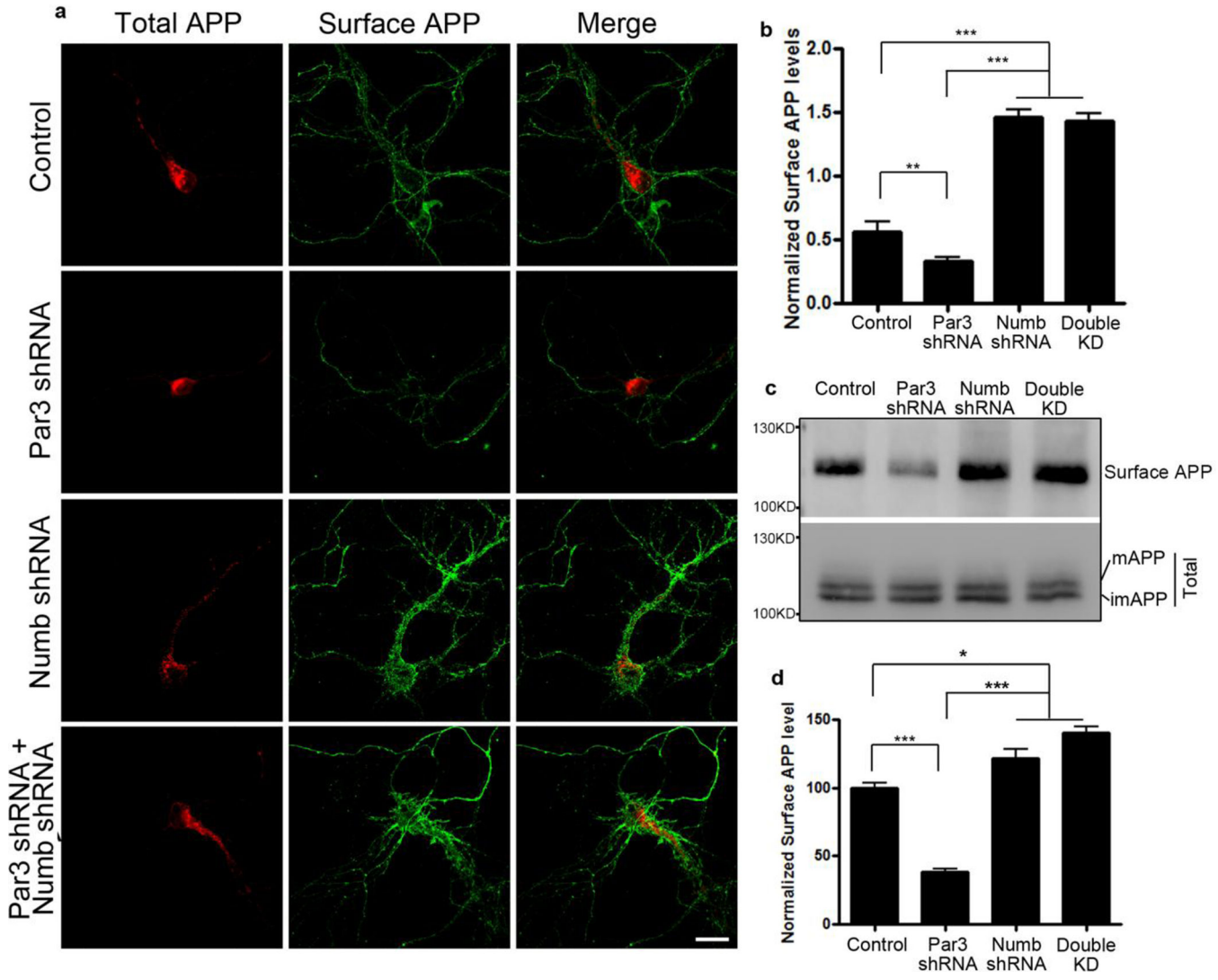

Figure 9. Knockdown of Numb rescues the decrease in surface APP in Par3-depleted neurons

(a) Primary hippocampal neurons were transfected with APP-RFP together with indicated constructs. Neurons were live labeled with APP 6E10 antibody to immunostain for surface APP (green).

(b) Quantification of surface APP level normalized to APP-RFP intensity. Data are expressed as Mean ± SEM with Student's t test, ** $p<0.01$, ***$p<0.001$, n=5–10. Scale bar: 10μm.

(c) APPwt N2a cells were transfected with the indicated constructs and surface biotinylated to measure surface APP levels. Biotinylated surface proteins were analyzed by Western blotting to reveal surface APP levels.

(d) Quantification of surface APP normalized to total APP, n=3. Data were expressed as Mean ± SEM with Student's t test: *$p<0.05$, *** $p<0.001$. Double KD: double knockdown of Numb and Par3.

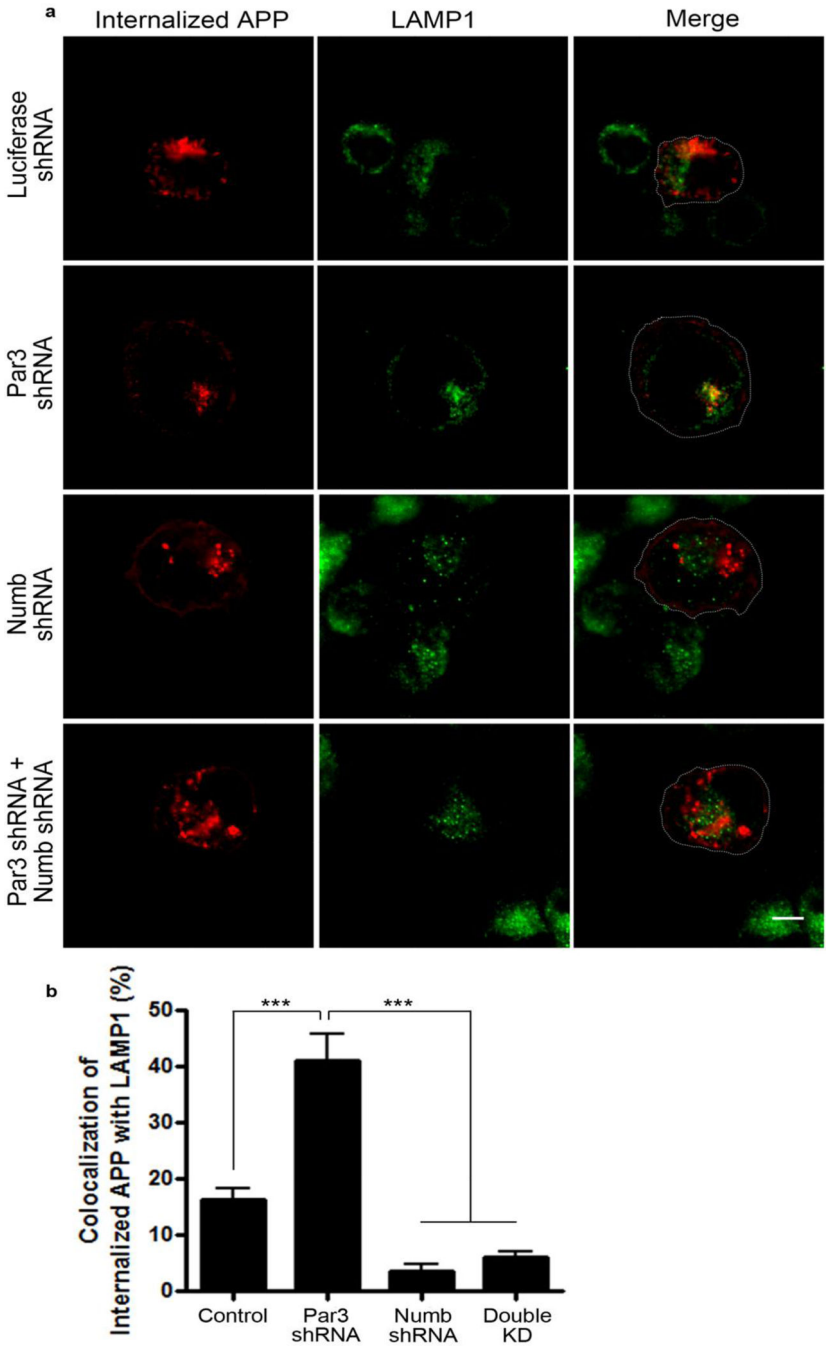

Figure 10. Knockdown of Numb reverses the lysosomal targeting of APP in Par3-depleted cells

(a) APPwt N2a cells were transfected with indicated constructs then live labeled with APP 6E10 antibody. Cells were fixed at 60 min after internalization and immunostained for internalized APP (red) and the lysosomal marker LAMP1 (green). Scale bar: 10μm.

(b) Quantification of colocalization between internalized APP and LAMP1. Data were expressed as Mean ± SEM with Student's t test, *** $p<0.001$. n=5–10. Double KD: double knockdown of Numb and Par3.

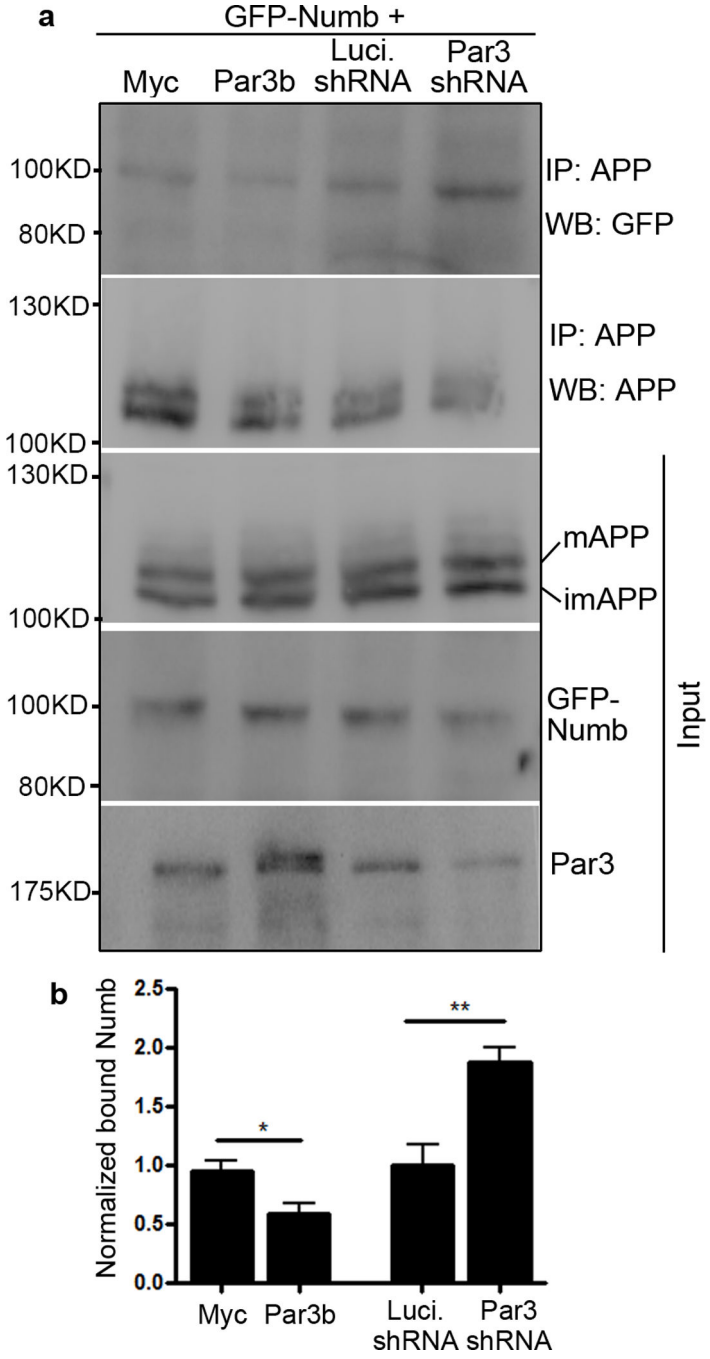

Figure 11. Par3 interferes with Numb-APP binding

(a) APPwt N2a cells were transfected with the indicated Par3 and Numb constructs. Cell lysates were immunoprecipitated with anti-APP 6E10 monoclonal antibody and immunoprecipitated complexes were analyzed by Western blot.

(b) Quantification of blots in (a), normalized to GFP-Numb input, *p<0.05, **p<0.01, n=3.